Chapter 63
A New Framework for the Assessment of Cerebral Hemodynamics Regulation in Neonates Using NIRS

Alexander Caicedo, Thomas Alderliesten, Gunnar Naulaers, Petra Lemmers, Frank van Bel, and Sabine Van Huffel

Abstract We present a new framework for the assessment of cerebral hemodynamics regulation (CHR) in neonates using near-infrared spectroscopy (NIRS). In premature infants, NIRS measurements have been used as surrogate variables for cerebral blood flow (CBF) in the assessment of cerebral autoregulation (CA). However, NIRS measurements only reflect changes in CBF under constant changes in arterial oxygen saturation (SaO_2). This condition is unlikely to be met at the bedside in the NICU. Additionally, CA is just one of the different highly coupled mechanisms that regulate brain hemodynamics. Traditional methods for the assessment of CA do not take into account the multivariate nature of CHR, producing inconclusive results. In this study we propose a newly developed multivariate methodology for the assessment of CHR. This method is able to effectively decouple the influences of SaO_2 from the NIRS measurements, and at the same time, produces scores indicating the strength of the coupling between the systemic variables and NIRS recordings. We explore the use of this method, and its derived scores, for the monitoring of CHR using data from premature infants who developed a grade III-IV intra-ventricular hemorrhage during the first 3 days of life.

Keywords Cerebral autoregulation • NIRS • Multivariable • Premature infants

A. Caicedo (✉) • S. Van Huffel
Department of Electrical Engineering (ESAT), STADIUS Center for Dynamical Systems, Signal Processing, and Data Analytics, KU Leuven, Leuven, Belgium

iMinds Medical IT, Leuven, Belgium
e-mail: acaicedo@esat.kuleuven.be

T. Alderliesten • P. Lemmers • F. van Bel
Department of Neonatology, University Medical Center, Wilhelmina Children's Hospital, Utrecht, The Netherlands

G. Naulaers
Neonatal Intensive Care Unit, University Hospitals Leuven, KU Leuven, Leuven, Belgium

C.E. Elwell et al. (eds.), *Oxygen Transport to Tissue XXXVII*, Advances in Experimental Medicine and Biology 876, DOI 10.1007/978-1-4939-3023-4_63

1 Introduction

Cerebral hemodynamics regulation (CHR) comprises a set of mechanisms that interact in order to maintain brain homeostasis [1]. These mechanisms are highly coupled and act upon sudden changes in systemic variables mitigating its effect on brain hemodynamics. In premature infants these mechanisms are likely to be impaired [2, 3]. Due to the fragility of the cerebral vascular bed in this population, monitoring CHR is of paramount importance in order to avoid brain damage. Near-infrared spectroscopy (NIRS) signals can be used in the continuous monitoring of CHR as markers for brain oxygenation. In addition, NIRS can also be used as surrogate variables for cerebral blood flow (CBF) and cerebral blood volume (CBV) [2, 3]. However, NIRS measurements are highly sensitive to changes in arterial oxygen saturation (SaO_2), which hinders their interpretation as a surrogate variable for both CBF and CBV. In the framework of CHR monitoring, this problem is avoided by performing the analysis in segments with relatively constant SaO_2. However, this condition is hardly met at the bedside in the neonatal intensive care units (NICU), hampering the introduction of CHR monitoring in clinical practice.

Additionally, most of the interest in this research field has been given to the monitoring of cerebral autoregulation (CA). CA is the mechanism that tries to maintain a proper CBF in the presence of changes in mean arterial blood pressure (MABP). This mechanism is described as a plateau region in the static relationship between MABP-CBF. Normal values of MABP are located inside the flat region of the CA curve. However, in the presence of hypotension/hypertension CBF might become pressure passive, which exposes the brain to damage due to ischemia or hemorrhage. In neonates, the upper and lower MABP thresholds of the CA plateau are unknown. In addition, these infants are likely to present low values of blood pressure. For this reason, these infants normally receive treatment for hypotension in order to avoid low cerebral perfusion. However, CA is not an isolated mechanism, there are several protection mechanisms that interact and affect the autoregulation curve. Metabolic influences caused by changes in blood gases concentration, as well as neurogenic activity, play an important role in the regulation of brain hemodynamics [1]. For this reason a multivariate approach for CHR monitoring is needed.

In this context, an appropriate CHR monitor should include measurements of MABP, partial pressure of CO_2 ($PaCO_2$) and a surrogate marker for neurogenic activity. For the latter, measurements of heart rate (HR) might be of particular interest, since they carry information about the sympathetic mediated and vagal outflow [4, 5]. In addition, measurements of SaO_2 should also be included in order to decouple its dynamics from NIRS measurements. The main goal in this paper is to highlight the importance of the use of multivariate models for the assessment of CHR, as well as the importance of a proper decoupling of physiological noise from the NIRS measurements.

2 Methods

Data For this study we used measurements from nine premature infants with a gestational age less than 32 weeks. From this population five subjects presented III-IV grade of intra-ventricular hemorrhage (IVH). The remaining four patients were matched controls. Concomitant measurements of HR, MABP, SaO_2 and regional cerebral oxygen saturation ($rScO_2$) measured by the INVOS 4100 (Somanetics, Troy, Michigan, USA) were obtained during their first 3 days of life. All data were recorded and stored in a personal computer using Poly 5 (Inspector Research Systems, Amsterdam, the Netherlands) with a sampling frequency of 1 Hz. Additionally, cranial ultrasound was performed daily in order to determine the presence of cerebral injury (e.g. white matter damage, IVH). These data are part of a large data collection presented in [6], and have also been used for a separate analysis in [7]. Figure 63.1 presents measurements from one representative subject.

Mathematical Tools We propose the use of a newly developed decomposition algorithm based on wavelet regression and oblique subspace projections (WR-OBP). In short, WR-OBP is a hybrid between wavelet regression and subspace system identification that uses input–output observations of the system in order to produce a mathematical model that can explain the measured output. Furthermore, WR-OBP is able to decouple the linked dynamics between the different underlying subsystems in order to decompose the observed output in terms of the partial contributions of each input variable. This is of considerable

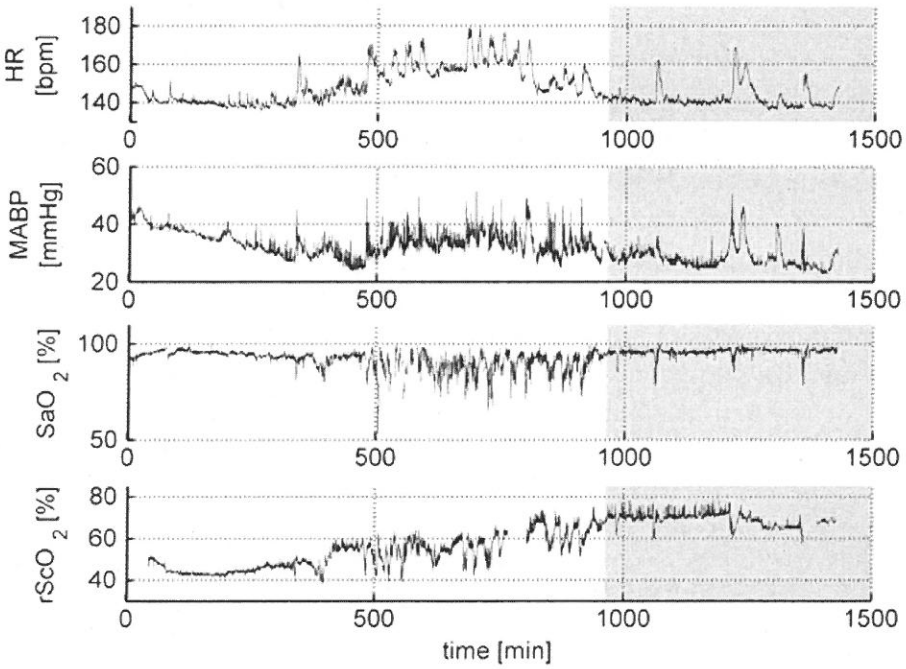

Fig. 63.1 Concomitant recordings of HR, MABP, SaO_2 and $rScO_2$ from a representative subject. The *shaded area* represents the interval of time between the last clinical evaluation with good outcome and the detection of a grade III IVH

interest in the framework of CHR monitoring, since it allows not only to decouple the influence of SaO_2 from the NIRS measurements, but also provides a set of signals that represent the time course relationship between each input variable and the respective output. This set of signals can be used to define scores for the assessment of the coupling between systemic and brain hemodynamic variables. A preliminary study using an early version of WR-OBP can be found in [8].

WR-OBP uses HR, MABP and SaO_2 as input variables and $rScO_2$ as the output of a mean average filter model of the form $y = Ax$. In order to construct the regression matrix A, the input variables are denoised using wavelet denoising and a block Hankel structured is formed with the denoised variables. The block Hankel matrix A, then, contains a set of delayed versions of the denoised input variables. The optimal number of delays is found by means of tenfold cross-validation. Once the linear regression has been solved, we used oblique subspace projections in order to find the contribution of each input variable in the $rScO_2$ changes. This can be interpreted as projecting the $rScO_2$ onto the signals subspaces of the input variables. In order to construct the oblique projectors, the columns of the regression matrix A that correspond to one of the input variables is used as the target subspace, while the rest of the columns are used as the reference subspace. The oblique projector is constructed using $P_{i.(i)} = A_i(A^T{}_i Q_{(i)} A_i)^{-1} A^T{}_i Q_{(i)}$, where $P_{i.(i)}$ is the oblique projection onto the input variable i along the reference subspace indicated by all the remaining variables, A_i is a partition of A containing only the columns related to the input variable i, $Q_{(i)} = I\text{-}P_{(i)}$, with $P_{(i)} = A_{(i)}(A^T{}_{(i)} A_{(i)})^{-1} A^T{}_{(i)}$ is the orthogonal projector onto the null space of the $A_{(i)}$, and $A_{(i)}$ the partition of A that remains after removing A_i. Finally, the contribution of the input variable I on the output is computed using $y_i = P_{i.(i)} y$.

Signal Processing We divided the signals in consecutive overlapping segments with a duration of 1000 s, and an overlapping of 500 s. For each segment we used MABP, HR and SaO_2 as inputs and $rScO_2$ as output in the WR-OBP decomposition algorithm. As a result, WR-OBP decomposed $rScO_2$ in three different signals, each one corresponding to one input variable, in such a way that $rScO_2 = (rScO_2)_{MABP} + (rScO_2)_{HR} + (rScO_2)_{SaO2} + \varepsilon$, with $(rScO_2)_i$ being the partial contribution of the variable i on the measured $rScO_2$ and ε an error component representing measurement noise and/or not modeled dynamics. The coupling coefficient between the output and a respective input variable was computed by dividing the power of the partial contribution of the respective input by the power of the output, e.g. the coupling coefficient between MABP-$rScO_2$ is computed as the ratio $Power[(rScO_2)_{MABP}]/Power[rScO_2]$. The decomposition of a representative segment of the measurements is shown in Fig. 63.2.

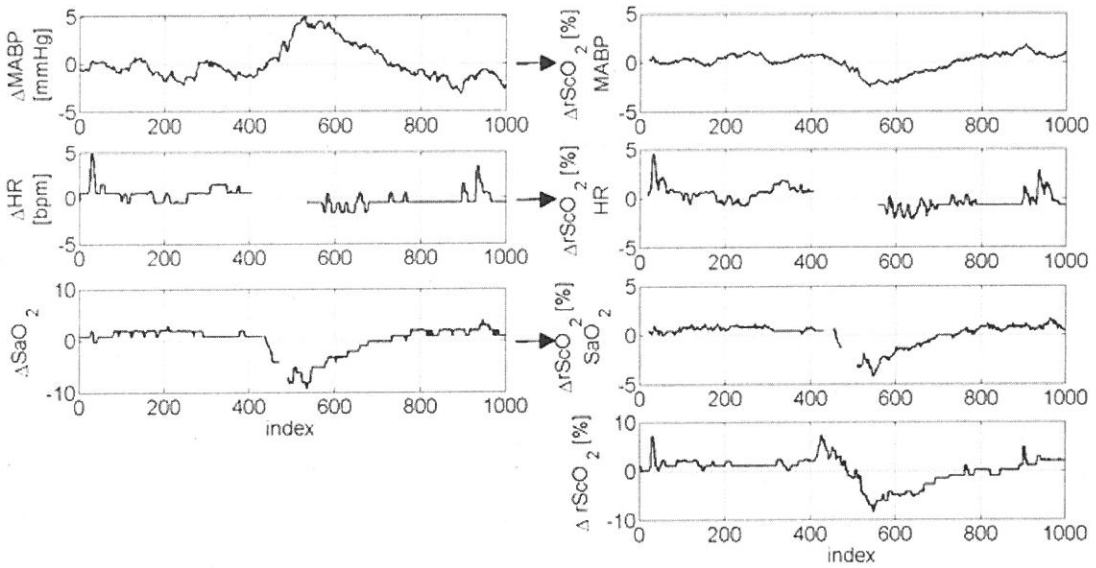

Fig. 63.2 Decomposition of a representative segment of the data using WR-OBP, on the *left* the input variables are displayed, from top to bottom MABP, HR and SaO_2. On the *right* the respective partial contribution of each input variable, as well as the measured output can be found. From *top* to *bottom* the contributions from MABP, HR, and SaO_2, the *last plot* represents the measured output, $rScO_2$

3 Results and Discussion

Figure 63.3 shows the results from WR-OBP applied to the measurements from the patient whose data are shown in Fig. 63.1. Since WR-OBP uses oblique projectors, and oblique projectors do not preserve the Euclidean norm, the coupling coefficients can be larger than 1. As a first approach to differentiate between control and IVH patients, in Fig. 63.4 we explored the dispersion of the scores using a scatter plot, where the x-axis represents the coupling coefficients between MABP-$rScO_2$ and the y-axis represents the coupling coefficients between HR-$rScO_2$. Furthermore, we divided the scores from the IVH-group in two subgroups, namely the pre-IVH region and the IVH region. We hypothesized that the scores of the pre-IVH region should behave similarly to the ones from the control group, while scores in the IVH region indicating the presence of an IVH episode should reflect the change in the coupling between systemic and hemodynamics variables. Since most of the data points for the control subjects and the pre-IVH sub-group were located in regions of low MABP-$rScO_2$ and/or HR-$rScO_2$ coupling, we propose to use the product of both coupling coefficients as a marker for IVH.

Figure 63.5 shows the time series with the product of the coupling scores for each subject who suffered an IVH. Interestingly, in all the patients, high coupling scores were found inside the shaded area, which represents the time interval between the last clinical evaluation with positive outcome and when the IVH was detected. We might hypothesize that the location in time of the high scores could be related to the onset of the IVH episode. However, we do not have the exact time

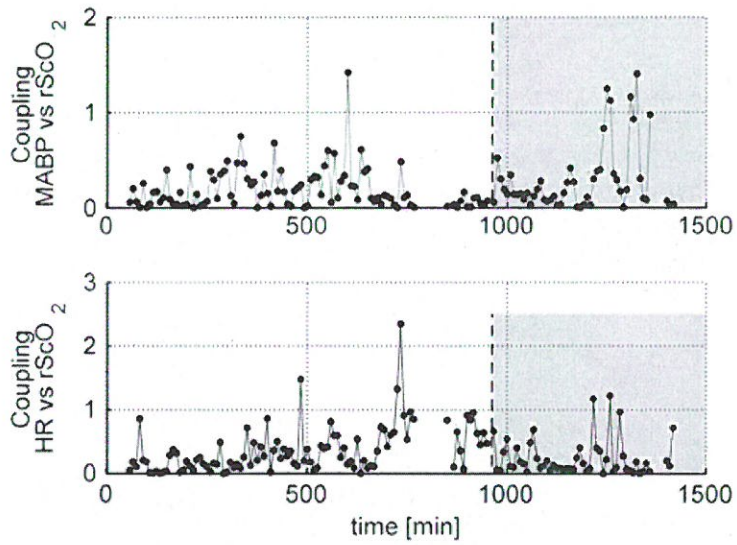

Fig. 63.3 Coupling coefficients between MABP-rScO$_2$ and HR-rScO$_2$ computed for a representative subject. The *shaded area* represents the time between the last clinical evaluation with positive outcome and the time when a grade III IVH was detected

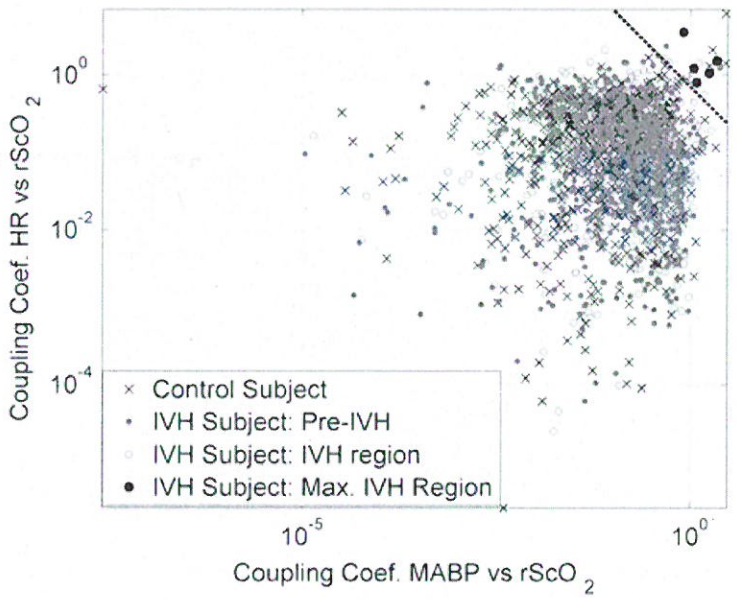

Fig. 63.4 Scatter plot of the coupling scores for CHR monitoring for all the subjects. The x-axis as we'll as the y-axis is in logarithmic scale. The *dashed line* indicate the limit of the boundary where the product of the coupling coefficients is lower than a selected threshold; this region is assumed to represent segments with low values of coupling between systemic and hemodynamics variables. The scores for the control subjects are plotted using 'x'. The scores for the IVH subjects are divided in two: pre-IVH region plotted using *grey dots*, and the region where the IVH occurred using *grey circles*. Finally, the *solid black circles* represent the segments that describe the maximum peaks in the IVH region

location of the episodes in order to prove this argument. Assuming this hypothesis as correct, just for illustrative purposes, we arbitrarily defined a threshold of 0.7 to identify the occurrence of an IVH event. Using this threshold, in Fig. 63.4 we plotted the area for which the product of the coupling coefficients was lower than this specified threshold. Additionally, we also marked in Fig. 63.4 the coupling coefficients corresponding to the segments with the maximum peaks in the IVH region found in Fig. 63.5. For subject 1 we took two peaks, since the maximum peak contains two data points.

The dispersion of the data in Fig. 63.4 indicates that, in the presence of a high coupling between systemic and cerebral hemodynamics, for some segments MABP dominates the changes in $rScO_2$, while in other segments HR drives the changes in $rScO_2$. This might indicate that the pathophysiology leading to the IVH could have differed between the patients. Therefore, looking only at one of the mechanisms involved in CHR might lead to inconclusive results. Additionally, in Fig. 63.4 some coupling coefficients corresponding to segments for the control group and the pre-IVH region can be found outside the normal (shaded) region. These segments with an apparent high coupling between systemic and hemodynamic variables produce false detections that might have been caused by the presence of artefacts, inaccuracies in the used algorithm, or unlabeled episodes of hemodynamic instability.

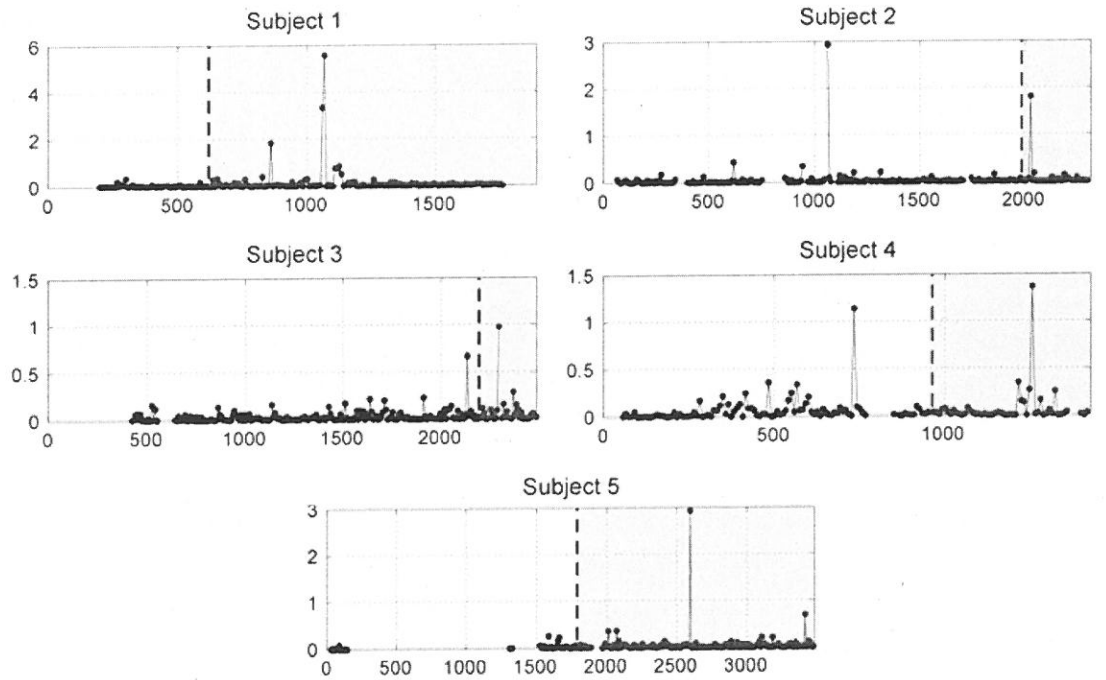

Fig. 63.5 Product of the coupling scores MABP-$rScO_2$ and HR-$rScO_2$ for the different subjects that suffered a grade III-IV IVH. The *shaded area* represents the time between the last clinical evaluation with positive outcome and the time when a grade III-IV IVH was detected. The y-axis represents the magnitude of the product of both scores, while the x-axis represents the time in minutes

We want to stress that the main goal of this paper is not to introduce a new marker for IVH, but to point out the importance of a multivariate framework for CHR monitoring. With the case study presented here we have found a promising relation between the results provided by our multivariate analysis and the possible detection of the onset of an IVH episode. However, several limitations should be taken into account. First, because the population included in the study is small, no strong conclusion can be drawn. Second, we only illustrate how a multivariate analysis can be used in the framework of CHR monitoring and how the results from this framework might be used to define markers for disease; however, these markers were not optimized, mainly due to the small population size and because the exact time of the IVH episode is unknown. The exact time of the IVH episode needs to be known in order to validate the proposed marker. However, despite the limitations of the study, these preliminary results are promising and highlight the importance of a multivariate framework for the monitoring of CHR using NIRS.

To conclude, we have presented a new framework for the assessment of CHR. This approach requires the use of multivariate models that are able to assess the influence of each measured systemic variable on brainhemodynamics. More importantly, this new framework suggests the need to study the information provided by the combined scores rather than studying their influences separately, to cope with inter-patient differences as well as differences in pathophysiology. Additionally, in a preliminary study, we showed that scores for CHR monitoring, obtained by combining the information of coupling between different systemic variables on brain hemodynamics, might be useful to detect the onset of IVH.

Acknowledgments Research supported by the Research foundation Flanders (FWO); Research Council KUL: GOA MaNet, CoE PFV/10/002 (OPTEC). Flemish Government: FWO: travel grant. Belgian Federal Science Policy Office: IUAP P719/(DYSCO), 'Dynamical systems, control and optimization', 2012–2017. Belgian Federal Science Policy Office: IUAP P7/19 DYSCO. EU HIP Trial FP7-HEALTH/2007–2013 (n° 260777).

References

1. Peng T, Rowley A, Plessis A et al (2000) Multivariate system identification for cerebral autoregulation. Ann Biomed Eng 36(2):308–320
2. Tsuji M, Saul J, du Plessis A et al (2000) Cerebral intravascular oxygenation correlates with mean arterial pressure in critically ill premature infants. Pediatr Rev 106(4):625–632
3. Wong F, Leung T, Austin T et al (2008) Impaired autoregulation in preterm infants identified by using spatially resolved spectroscopy. Pediatrics 121:604–611
4. Purkayastha S, Saxena A et al (2012) α_1-Adrenergic receptor control of the cerebral vasculature in humans at rest and during exercise. Exp Physiol. doi:10.1113/expphysiol.2012.066118
5. Schaffer L, Burkhardt T et al (2008) Cardiac autonomic balance in small-for-gestational-age neonates. Am J Physiol Heart Circ Physiol 294:H884–H890
6. Alderliesten T, Lemmers P et al (2013) Cerebral oxygenation, extraction, and autoregulation in very premature infants who develop peri-intraventricular hemorrhage. J Pediatr 162(4):698–704

7. Caicedo A, Varon C et al (2014) Differences in the cerebral hemoynamics regulation mechanisms of premature infants with intra-ventricular hemorrhage assessed by means of phase rectified signal averaging. In: Proceedings of the IEEE EMBC 2014, Chicago, 4208–4211 pp
8. Caicedo A, Tachtsidis I et al (2012) Decoupling the influence of systemic variables in the peripheral and cerebral haemodynamics during ECMO procedure by means of oblique and orthogonal subspace projections. In: 2012 Annual international conference of the IEEE Engineering in Medicine and Biology Society (EMBC), 6153–6156 pp